

Trehalose-Based Block Copolymer Promote Polyplex Stabilization for Lyophilization and in Vivo pDNA Delivery

Zachary P. Tolstyka,[†] Haley Phillips,[†] Mallory Cortez,^{†,‡} Yaoying Wu,^{†,§} Nilesh Ingle,[†] Jason B. Bell,[†] Perry B. Hackett,[†] and Theresa M. Reineke^{*†}

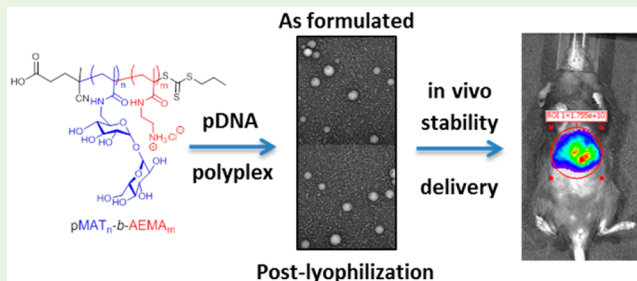
[†]Department of Chemistry and Center for Genome Engineering, University of Minnesota, 207 Pleasant Street SE, Minneapolis, Minnesota 55455, United States

[‡]Department of Genetics, Cell Biology and Development, and Center for Genome Engineering, University of Minnesota, Minneapolis, Minnesota 55455, United States

S Supporting Information

ABSTRACT: The development and thorough characterization of nonviral delivery agents for nucleic acid and genome editing therapies are of high interest to the field of nanomedicine. Indeed, this vehicle class offers the ability to tune chemical architecture/biological activity and readily package nucleic acids of various sizes and morphologies for a variety of applications. Herein, we present the synthesis and characterization of a class of trehalose-based block copolymers designed to stabilize polyplex formulations for lyophilization and in vivo administration. A 6-methacrylamido-6-deoxy trehalose (MAT) monomer was synthesized from trehalose and polymerized via reversible addition–fragmentation chain transfer (RAFT) polymerization to yield pMAT₄₃. The pMAT₄₃ macro-chain transfer agent was then chain-extended with aminoethylmethacrylamide (AEMA) to yield three different pMAT-*b*-AEMA cationic-block copolymers, pMAT-*b*-AEMA-1 (21 AEMA repeats), -2 (44 AEMA repeats), and -3 (57 AEMA repeats). These polymers along with a series of controls were used to form polyplexes with plasmids encoding firefly luciferase behind a strong ubiquitous promoter. The trehalose-coated polyplexes were characterized in detail and found to be resistant to colloidal aggregation in culture media containing salt and serum. The trehalose-polyplexes also retained colloidal stability and promoted high gene expression following lyophilization and reconstitution. Cytotoxicity, cellular uptake, and transfection ability were assessed in vitro using both human glioblastoma (U87) and human liver carcinoma (HepG2) cell lines wherein pMAT-*b*-AEMA-2 was found to have the optimal combination of high gene expression and low toxicity. pMAT-*b*-AEMA-2 polyplexes were evaluated in mice via slow tail vein infusion. The vehicle displayed minimal toxicity and discouraged nonspecific internalization in the liver, kidney, spleen, and lungs as determined by quantitative polymerase chain reaction (qPCR) and fluorescence imaging experiments. Hydrodynamic infusion of the polyplexes, however, led to very specific localization of the polyplexes to the mouse liver and promoted excellent gene expression in vivo.

KEYWORDS: glycopolymer, nanoparticle, nanomedicine, nonviral gene delivery, stealth polymer, transfection, RAFT polymerization, hydrodynamic injection, cryo-stabilization



INTRODUCTION

Gene therapy offers new avenues for the treatment of genetic diseases characterized by deficiency of a protein that can be treated by the delivery of DNA encoding the required polypeptide.^{1–8} Viral vectors are often used for DNA delivery; however, the most commonly used viruses have limited DNA cargo capacity and many elicit strong immunological responses. In contrast, nonviral vectors can package any length of nucleic acid; however, delivery of nonviral vectors into cells is generally very difficult to achieve at levels that have therapeutic efficacy.¹²

Cationic polymers that form an interpolyelectrolyte complex with the negatively charged phosphodiester backbone of DNA or RNA,¹³ termed polyplexes, are an attractive choice for nonviral gene delivery agents as their chemical structure, functionality,

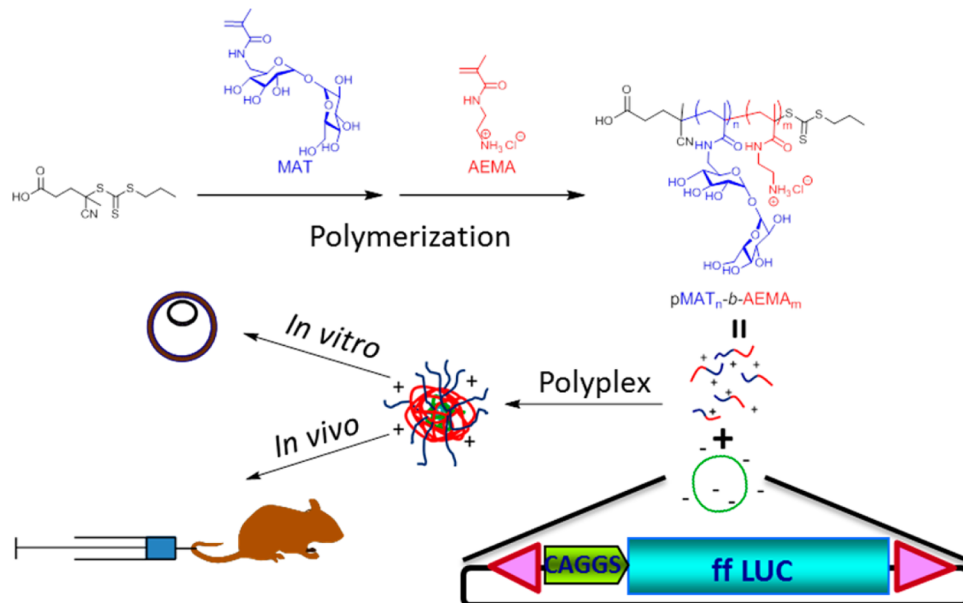
and molecular weight can be tailored in a controlled fashion. Typically, polyplexes contain an excess of polymer, which yields a complex that has a net positive charge. However, when such polyplexes are introduced into the bloodstream they aggregate with various negatively charged proteins, which hinders their ability to penetrate the plasma membranes of cells in tissues.¹⁴ Therefore, noncharged “stealth” coatings such as polyethylene glycol (PEG) have been used to help shield these particles from aggregation.¹⁵ PEGylated complexes generally have decreased immunogenicity and increased lifetimes in the blood when

Received: July 22, 2015

Accepted: November 20, 2015

Published: December 22, 2015

Scheme 1. Polymerization 6-methacrylamido-6-deoxy-trehalose (MAT) and N-(2-aminoethyl)methacrylamide (AEMA) Yields a Series of pMAT-*b*-AEMA Delivery Vehicles^a



^aThese trehalose-based block copolymers were mixed with plasmid DNA (pDNA, shown in detail in the inset) to form polyplexes that were examined both in vitro and in vivo.

compared with their unmodified counterparts.^{16,17} However, PEG is nonbiodegradable and has been implicated in antibody formation,¹⁷ hypersensitivity reactions^{18,19} and accelerated blood clearance upon repeated dosage.^{20–22} Accordingly, we have focused on building novel carbohydrate-based polymers to create a hydrophilic polyplex shell as an alternative to PEG. This study presents the first systematic investigation of these glycopolymers *in vivo*.

Previously, we polymerized the glucose-based monomer, 2-deoxy-2-methacrylamido glucopyranose (MAG), to form a block copolymer with *N*-(2-aminoethyl) methacrylamide (AEMA).²³ Tests *in vitro* suggest that the cationic glycopolymers have superior solution stability and lower cell toxicity in cell culture compared to polyethylenimine (PEI) complexes. The use of trehalose has also recently been explored as a PEG alternative.²⁴ Trehalose is an α - α -linked dimer of glucose that is synthesized by bacteria, fungi, plants, and invertebrate animals^{25,26} and used by living systems to survive in extreme conditions.^{27,28} Trehalose has long been used as a stabilizing agent in drug formulations such as Herceptin and Lucentis.²⁹ Step-growth polymers have been synthesized using a modified trehalose as one of the monomers. Polyplexes formed with these polymers have been found to display lower toxicity, high cellular uptake, and similar gene expression when compared to the commercially available gene delivery polymer jetPEI.^{30–32} Polytrehalose has been shown to impart thermal stability to proteins: lysozyme enzymatic activity was retained upon extreme heating and cooling when polytrehalose was covalently attached.³³ Our lab has reported polyplexes formulated with short interfering RNA (siRNA) and a trehalose block copolymer 6-methacrylamido-6-deoxy trehalose-*co*-*N*-(2-aminoethyl) methacrylamide (pMAT-*b*-AEMA).²⁴ Polyplexes formulated with pMAT-*b*-AEMA polymers displayed high uptake efficiency and powerful gene knockdown in U87 cells.²⁴

Herein, we investigate the use of pMAT-*b*-AEMA block copolymers in the formulation of polyplexes containing pT2/Cal plasmid DNA (pDNA) for gene delivery *in vitro* and *in vivo* (Scheme 1). These plasmids contain a *Sleeping Beauty* transposon

carrying the firefly luciferase reporter gene under the regulation of a strong synthetic promoter (CAGGS) that is highly active in vertebrate cells.³⁴ Delivery experiments were first performed in cultured glioblastoma (U87) and human liver carcinoma (HepG2) cell lines and found to be highly efficacious. The trehalose polymers were then examined for the ability to stabilize polyplex formulations through lyophilization and reconstitution. We reveal that these trehalose-coated polyplexes retain pDNA delivery and gene expression activity after lyophilization and reconstitution, an important metric to improve the consistency of gene delivery and increase shelf life of nanomedicines. We also reveal the first examination of these trehalose block copolymers for *in vivo* pDNA administration. Polyplex formulations were administered to mice using two different injection techniques to observe toxicity, biodistribution, and efficacy of gene delivery *in vivo*. We reveal that these trehalose-coated polyplexes shield the formulations from nonspecific tissue internalization under slow tail vein infusion, yet also retain stability *in vivo* following rapid hydrodynamic injection, resulting in the promotion of highly specific and excellent gene expression in the mouse liver (compared to JetPEI and pDNA only controls). Indeed, this study demonstrates that trehalose-coated nanomedicines offer a new stealth design motif that could provide an alternative to PEGylation for stabilizing formulations for *in vivo* administration.

MATERIALS AND METHODS

A brief version of the material and methods used is provided here. More detailed methods are included in the Supporting Information.

Materials. All reagents were obtained at the highest available purity from Thermo Fisher Scientific, Inc. (Pittsburgh, PA) or Sigma-Aldrich Co. LLC. (St. Louis, MO) and used as received unless noted otherwise. JetPEI was obtained from Polyplus-transfection SA (Illkirch, France). Glycofect was obtained from Techulon, Inc. via donation. 6-Methacrylamido-6-deoxy trehalose (MAT) was synthesized as described previously.²⁴ Propidium iodide, UltraPure Agarose-1000, trypsin, (3-(4,5-dimethylthiazol-2-yl)-2,5-diphenyl tetrazolium bromide (MTT), phosphate-buffered saline (PBS), Minimum Essential Medium

with reduced serum (Opti-MEM) and Dulbecco's Modified Eagle Medium (DMEM) were purchased from Life Technologies – Thermo Fisher Scientific (Carlsbad, CA). The pT2/CaL plasmid was prepared as described previously.³⁵ The Luciferase Assay Kit and cell lysis buffer were obtained from Promega Corporation (Madison, WI). Bio-Rad DC Protein Assay Reagent A, Reagent B and Reagent S were obtained from Bio-Rad Laboratories, Inc. (Hercules, CA). HepG2 and U87 cells were obtained from the American Type Culture Collection (ATCC) (Manassas, VA). The cells were grown in complete DMEM [supplemented with 10% (v:v) fetal bovine serum and 1% antibiotic-antimycotic solution (containing penicillin, streptomycin, and amphotericin B)] at 37 °C and 5% CO₂ in a humidified incubator.

Wild-type (WT) C57BL/6J 6wk-old mice were purchased from Jackson Laboratories (Sacramento, CA). All mice were maintained under AAALAC-accredited (Association for Assessment and Accreditation of Laboratory Animal Care) specific pathogen-free conditions.

Instrumentation. NMR spectra were recorded using a Bruker Avance III HD 500 MHz spectrometer in D₂O purchased from Cambridge Isotope Laboratories, Inc. (Andover, MA). NMR data was analyzed using Bruker Top Spin version 3.1. UV-vis data was collected with an Ocean Optics Inc. CUV 1 cm cuvette holder powered by a Mikropack DH-2000 Deuterium/Halogen open-close TTC lamp, and data was analyzed by Ocean Optics Inc. Basic Acquisition Software.

Size exclusion chromatography (SEC) was conducted using an Agilent 1260 High Performance Liquid Chromatograph running 1.0 wt % acetic acid/0.1 M Na₂SO₄ as the eluent at a flow rate of 0.4 mL/min on size exclusion chromatography columns [CATSEC1000 (7 μ, 50 × 4.6), CATSEC100 (5 μ, 250 × 4.6), CATSEC300 (5 μ, 250 × 4.6), and CATSEC1000 (7 μ, 250 × 4.6)] obtained from Eprogen Inc. (Downers Grove, IL). Signals were acquired using Wyatt HELEOS II light scattering detector ($\lambda = 662$ nm), and an Optilab rEX refractometer ($\lambda = 658$ nm). SEC trace analysis was performed using Astra VI software (version 5.3.4.18), Wyatt Technologies (Santa Barbara, CA). The hydrodynamic diameters of the polyplexes were recorded via dynamic light scattering measurements (DLS) with a Malvern Zetasizer Nano ZA. MTT, protein, and luciferase assay plates were analyzed using a Biotek Synergy H1 plate reader (BioTek Instruments, Inc., Winooski, VT). Cy5-uptake was measured on a FACSVerse (Becton Dickinson Biosciences, San Jose, CA) flow cytometer. TEM images were obtained with a FEI Tecnai G2 Spirit BioTWIN (FEI, Hillsboro, OR) transmission electron microscope, operated at 120 kV.

Live animal and animal tissue imaging were performed on an IVIS Spectrum In Vivo Imaging system and data was analyzed with the Living Image software (PerkinElmer Inc., Waltham, MA). RT-qPCR was performed using an Eppendorf Mastercycler (software version 2.2; Eppendorf).

Polymer Synthesis and Polyplex Characterization. *Synthesis of Poly(methacrylamidotrehalose) (pMAT₄₃)*. PMAT₄₃ was synthesized as previously described.²⁴ Briefly, MAT monomer was polymerized via RAFT in acetate buffer. 4-cyano-4-(propylthiocarbonothioylthio)-pentanoic acid was dissolved in 645 μL of MeODH and added to the MAT solution, followed by 4,4'-azobis(4-cyanovaleic acid) (V-501). Finally, 861 μL of MeOD was added and oxygen was removed by bubbling nitrogen through the system for 45 min. The flask was heated to 70 °C for 6 h and the reaction was stopped by removing the septum and cooling the reaction mixture on ice. The polymer solution was dialyzed against ultrapure water (3500 Da MWCO) and acidified to pH 4–5 with HCl. After 3 d of dialysis, the polymer solution was freeze-dried on a VirTis benchtopK lyophilizer at 62 mT with the condenser at -57.4 °C to yield 454 mg of white solid. Method details and characterization results can be found in Figure S1.

Synthesis of Cationic Diblock Copolymers pMAT-b-AEMA-1, -2, and -3. Cationic diblock copolymers were synthesized as previously reported.²⁴ Briefly, pMAT₄₃ and V-501 were dissolved in 1.0 M acetate buffer (pH 5.5) and added to a Schlenk tube containing aminoethylmethacrylamide hydrochloride (AEMA). Deoxygenation was achieved via bubbling nitrogen gas for 45 min. The tube was heated to 70 °C. Aliquots (1.25 mL) were removed via syringe at 30 min (pMAT-b-AEMA-1) and 60 min (pMAT-b-AEMA-2). Each aliquot was exposed to air and cooled in liquid nitrogen to stop polymerization.

After 90 min (pMAT-b-AEMA-3), the reaction was halted by septum removal and submerging the Schlenk tube in liquid nitrogen. All three copolymers were dialyzed (3500 Da MWCO) against 0.5 M NaCl solution, followed by 0.1 M NaCl and finally ultrapure water. All dialysis media were acidified with HCl to pH 4–5. Polymer solutions were lyophilized as described above to yield white, flocculent powders. All experiments were completed using polymers pMAT-b-AEMA-1, -2, and -3. Polymer characterization details can be found in Figures S2–S5.

Synthesis of Cy7-pMAT-b-AEMA-2. PMAT-b-AEMA-2 was labeled using an NHS-Cy7 fluorophore by dissolving it in H₂O. Cy7 functionalized with N-hydroxysuccinamide (NHS-Cy7) in DMF was added followed by DMF to target 1 fluorophore/50 amine residues. The mixture was vortexed for 30 s and allowed to proceed at room temperature for 4 h in the dark. The labeled polymer was purified via dialysis (3500 MWCO) against H₂O (acidified to pH ~5.5 with HCl) for 2 days and lyophilized using the same conditions listed before to yield blue flocculent solid.

Extent of labeling was quantified by measuring the absorbance of a 0.2 mg/mL solution of labeled polymer in H₂O at 750 nm via UV-vis ($\epsilon = 199000$ at 750 nm, Abs = 0.16), giving approximately 1 Cy7 fluorophore/10 polymer chains (Figure S6).

Polyplex Formation for Gel Electrophoresis and Tissue Culture (In Vitro) Experiments. Polymer solution at an appropriate concentration in water was added to a 400 μM solution of pDNA in DNase/RNase-free distilled water in an equal volume to yield polyplexes of (nitrogen to phosphate ratios) N/P = 7, 14, and 21 at a final concentration of 200 μM pDNA. The nitrogen ratios were calculated based on the concentrations of amines (either pendant from AEMA blocks or within the backbone of jetPEI or Glycofect). The solutions were incubated at 23 °C for 1 h before further use.

Gel Electrophoresis. A gel electrophoresis mobility shift assay was run to determine the minimal amount of polymer needed to achieve complete binding of the pDNA. Ten μL of each polyplex solution formulated at various N/P ratios were diluted with 10 μL of water to achieve a concentration of 100 μM and were incubated at 25 °C for 1 h to allow polymer-pDNA binding. The polyplex suspensions were run on agarose gels (0.6%) containing 6 μg ethidium bromide at 60 V for 80 min. Images were obtained using 312 nm UV light (Figure S7).

Dynamic Light Scattering (DLS). To measure polyplex size in a protein environment over time, we ran DLS experiments in DMEM containing 10% FBS. Polyplexes were formulated at N/P = 7, 14, and 21 in H₂O and incubated for 1 h at a concentration of 200 μM pDNA (to allow complexation) before being diluted with DMEM containing 10% FBS by volume. For DLS studies prior to lyophilization, the polyplexes were diluted to a final concentration of 100 μM ($T = 0$ h). For the postlyophilization DLS, polyplexes were prepared and lyophilized as previously described, reconstituted with water for 1 h, then diluted with DMEM with 10% FBS to 133 μM. Size measurements were taken at 25 °C using a 173° detection angle at times of 0, 1, 2, and 4 h (Figure S8).

Transmission Electron Microscopy (TEM) Imaging. Three μL of polyplex solution (formulated with pDNA and polymers pMAT-b-AEMA-1, -2, or -3) prepared at N/P = 10 were applied to a 300-mesh carbon coated copper grid (Ted Pella, Inc., Redding, CA) and negatively stained with uranyl acetate. Images were saved as TIFF files and polyplexes sized (excluding polyplexes on image edges) by counting pixels using Microsoft Paint, and the sizes are plotted in Figure S9.

Examination of Polyplex Function In Vitro. MTT Assay. MTT (3-(4, 5-dimethylthiazol-2-yl)-2, 5-diphenyltetrazolium bromide) was used to estimate the cytotoxicity of the polyplexes. HepG2 or U87 cells were seeded at 50 000 cells/well in 24-well plates 24 h prior to transfection. Polyplexes were formulated as described previously, then mixed with transfection media (200 μL of either OptiMEM (Figure S10) or DMEM containing 10% FBS). The mixture was added to each well. The transfection was ended 4 h later by diluting polyplexes with 1 mL of complete DMEM containing 10% FBS. 48 h after polyplexes were added to the cells, 0.5 mg/mL of MTT was added to each well and incubated for 1 h. Cells were lysed using DMSO and 200 μL aliquots were transferred to a 96-well plate for analysis using the plate reader (absorbance was measured at 570 nm). Nontransfected cells were used for normalizing the data.

Cellular Uptake Assay. Flow cytometry experiments were performed to examine the cellular uptake of Cy5-labeled pDNA 4 h post-transfection. HepG2 or U87 cells were seeded at 300 000 cells/well in 6-well plates 24 h prior to transfection. Polyplexes were prepared as described in the MTT assay protocol, except that the formulation was scaled up from 50 000 cells to 300 000 cells. After 4 h, the polyplex media was removed and cells were detached from the plate surface using trypsin, centrifuged to remove polyplexes and trypsin, and then washed twice with PBS. Finally, 1 mL of PBS was added and the cellular suspensions were kept on ice. Propidium iodide (1.0 mg/mL, 2.5 μ L) was added prior to analysis. Each experiment was performed in triplicate, and OptiMEM results are plotted in Figure S11.

Luciferase Gene Expression. Cells (HepG2 and U-87) were seeded at 50 000 cells/well in 24-well plates 24 h prior to transfection. Polyplexes were prepared, diluted, and applied to the cells as described in the cytotoxicity section above. After 48 h, the cells were washed with PBS and treated with cell lysis buffer. Aliquots (5 μ L) of cell lysate combined with 100 μ L luciferase substrate were examined in 96-well plates using a luminometer to determine relative light units (RLUs). Data were measured in triplicate and normalized for the amount of protein in each sample. Sample averages were plotted with error bars representing standard deviations (OptiMEM results in Figure S12).

Mouse Studies. Tail Vein Injections. Appropriate amounts of polyplexes (10 μ g or 25 μ g of pDNA/dose at desired N/P of polymer) were prepared in a 5% by weight aqueous dextrose solution (D₅W, Hospira, Inc.), and a 200 μ L dose of polyplexes was injected through the tail vein of experimental animals. After injection, animals were returned to their colony and imaged after 24 and 48 h. Mice injected with Cy7-labeled polymer were imaged immediately (data not shown), euthanized, and then their organs were imaged ex vivo.

Hydrodynamic Injections. Appropriate amounts of polyplexes (10 μ g or 25 μ g of pDNA/dose at desired N/P of polymer) were prepared in D₅W solution and injected through the tail vein of experimental animals using a hydrodynamics-based procedure as previously described.³⁶ Briefly, animals to be injected were weighed. A polyplex solution with a volume equivalent to 10% of the weight of the mouse was injected in 3 to 4 s. After injection, animals were placed on a heating pad to recover, then returned to their colony. Mice were either imaged for luciferase transgene expression about 24 and 48 h after transfection or imaged immediately after injection for Cy7 polymer fluorescence. After fluorescence imaging, mice were euthanized and their organs were imaged ex vivo.

Bioluminescence Imaging In Vivo. One hundred microliters of luciferin substrate solution (28.5 mg/mL) was injected intraperitoneally to each mouse. Three to five minutes later, mice were imaged for 1 min using a Xenogen Spectrum CCD camera system (Xenogen, Alameda, CA) according to the manufacturer's instructions. Each experiment was performed in triplicate.

Euthanizing and Tissue Collection/Processing. Mice were euthanized by carbon dioxide (CO₂) inhalation, perfused with saline, and selected organs were resected and preserved for analyses. Plasma and tissues were stored at -80 °C. Frozen tissues were homogenized by mortar and pestle, and ~100 mg of each tissue sample was removed for DNA processing. DNA was pulled from the organs using a phenol-chloroform extraction and ethanol precipitation. DNA purity and concentration were determined by using a NanoDrop instrument (Thermo Scientific, Wilmington, DE).

qPCR. DNA samples were normalized to 100 ng/ μ L. Five hundred nanograms of DNA was used with TaqMan Gene Expression Master Mix (Life Technologies – Thermo Fisher Scientific, Carlsbad, CA). TaqMan primers were designed and manufactured by Life Technologies – Thermo Fisher Scientific (Carlsbad, CA), Custom Plus TaqMan Assay, Assay ID – AJ6RNJ4. A standard curve was prepared by serially diluting pT2/CaL plasmid into WT C57BL/6 DNA. Samples were run using the impulse setting. The following conditions were used for the qPCR experiments: 95 °C for 10 min and 40 cycles of 90 °C for 15 s then 60 °C for 1 min.

Statistical Analysis. Statistical analysis was performed using JMP Pro Software (SAS Institute, Cary, NC) through the University of Minnesota Supercomputing Institute.

RESULTS AND DISCUSSION

Polymer Synthesis and Polyplex Characterization.

Trehalose is a carbohydrate with unique cryo- and lyo-protectant properties, which have prompted the use of this carbohydrate in materials synthesis to both retain and enhance these protective abilities.^{24–28,37} Previously, we have shown that trehalose-containing block copolymers are effective in the formulation of polyplexes and efficient delivery of siRNA.²⁴ Herein, we sought to examine these trehalose-based polycations for delivery of plasmids to cells in culture and in organs of living animals. Trehalose-based polymers were synthesized via reversible-addition–fragmentation chain-transfer (RAFT) polymerization with a 65:1 monomer: chain-transfer agent (CTA) ratio of 6-methacrylamido-6-deoxy methacrylamido trehalose (MAT) and 4-cyano-4-(propylthiocarbonothioylthio)-pentanoic acid (CPP) with 4,4'-azobis(4-cyanovaleric acid) (V-501) as the initiator to yield pMAT with 43 repeats. This 43-repeat unit pMAT was used as a macro CTA and chain-extended via RAFT polymerization with 125 equiv of N-(2-aminoethyl) methacrylamide (AEMA) and V-501 as the initiator to yield three cationic block copolymers (Table 1),²⁴ pMAT-*b*-AEMA-1 (21 repeats), -2 (44 repeats), and -3

Table 1. Polymer Structure and Molecular Weight

polymer	MAT repeat units	AEMA repeat units	mol wt (kDa)	D
pMAT- <i>b</i> -AEMA-1	43	21	20.4	1.07
pMAT- <i>b</i> -AEMA-2	43	44	23.3	1.07
pMAT- <i>b</i> -AEMA-3	43	57	25.0	1.08

(57 repeats), with each having the same length of MAT block but increasing lengths of the AEMA block.

These polymers were combined with pDNA encoding for the luciferase reporter gene to form polyplexes. The amount of polymer needed to fully bind the pDNA was first determined via gel electrophoresis. Polymers and pDNA were mixed at nitrogen-to-phosphate (N/P) ratios of 1, 2, 3, 4, 5, and 10, mixed with 1 μ L of running buffer and electrophoresed through a 0.6% w/w agarose gel containing ethidium bromide in TAE buffer. The gel was imaged under UV light to confirm binding (Figure S7). Anionic plasmid that remains uncomplexed by the cationic polymer migrates through the gel toward the positively charged anode whereas fully complexed DNA does not. All three polymers fully bound the DNA at N/P = 3. For further studies, each polymer was combined with DNA at three different N/P ratios: 7, 14, and 21, yielding nine polyplex formulations. Polyplex size and stability from aggregation in biological media containing serum (10% by volume fetal bovine serum, FBS) were examined via dynamic light scattering (DLS). We have previously shown that polyplexes formed from this polymer and siRNA have a positive ζ -potential in H₂O. Polyplexes were formulated at 200 μ M pDNA and allowed to complex for 1 h at 23 °C in water. The polyplexes were then diluted with Dulbecco's Modified Eagle Medium (DMEM) containing 10% by volume fetal bovine serum (FBS) solution to a final concentration of 100 μ M in pDNA, and the polyplex size was monitored over 4 h (Figure 1). ζ -potential of these polyplexes was not collected as the presence of FBS disrupts the measurement.

Trehalose polyplex size (~50–100 nm in diameter) remained consistent over the course of this experiment relative to the control polyplexes, jetPEI (N/P = 5) and Glycofект (N/P = 20), which increased in diameter with time. It is proposed that the jetPEI and Glycofект polyplexes aggregate with amino acids,

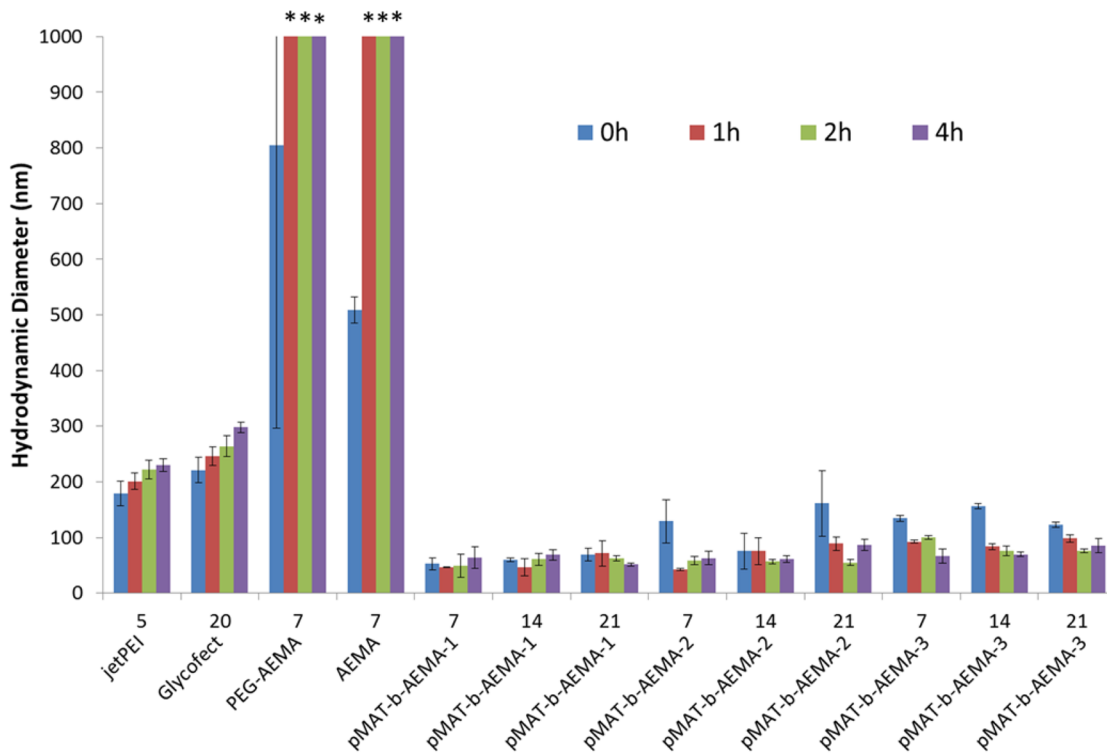


Figure 1. Polyplex size in DMEM containing 10% FBS monitored at an initial formulation of 200 μM in water and diluted to 100 μM in DMEM containing 10% FBS (0 h), and at 1, 2, and 4 h post dilution. The numbers on the x-axis indicate the N/P of the sample. The error bars represent standard deviation of triplicate measurements. Polyplexes that were very large and beyond the upper detection limit of our DLS instrument were marked with an asterisk (*).

buffer salts, and FBS proteins found in DMEM, which neutralizes their surface charge and causes aggregation. The trehalose polyplexes neither aggregate nor swell compared to the control complexes. This result mirrors what has been observed previously with carbohydrate-based block-*co*-polycations: poly 2-deoxy-2-methacrylamido glucopyranose-*b*-N-(2-aminoethyl) methacrylamide (pMAG-*b*-AEMA) polyplexes formulated with pDNA²³ and pMAT-*b*-AEMA polyplexes formulated with siRNA.²⁴ Polyplexes formed with cationic polymers containing a carbohydrate block are protected from aggregation. The pendant trehalose units of the MAT portion of the block copolymer likely form a shell around the outside of the polymer-pDNA polyplex, providing a highly hydrophilic layer and facilitating steric stabilization of the polyplexes in biological media.

To examine further the polyplex formulations, we used transmission electron microscopy (TEM) to image the formulations before and after lyophilization. Each of the polymers (pMAT-*b*-AEMA-1, -2, or -3) were mixed and allowed to complex with pDNA at N/P = 10 in water for 1 h at 23 °C, then the sample was divided into two portions. The first portion was imaged by TEM immediately (Figure 2a–c), whereas the second was lyophilized and resuspended before imaging (Figure 2d–f).

No significant size or shape differences were observed between the fresh polyplexes and those reconstituted following lyophilization. We have recently reported that polyplexes formed with pMAT-*b*-AEMA and siRNA maintained size and biological activity following lyophilization and resuspension. The particles appear slightly smaller in the TEM images than via DLS, likely due to a combination of dehydration of the particles during TEM sample preparation³⁸ and the preference of the negative stain for the highly charged core of the particle.³⁹

Examination of Polyplex Function In Vitro. Examination of the polyplex function was performed on two human cell lines with differing physiological function to assess the general biologic activity of the polyplex formulations. Cell culture studies of polyplex internalization and luciferase gene expression were performed in both HepG2 liver carcinoma and U87 glioblastoma human cell lines. We chose to examine two cell lines as we have found polyplex behavior to vary substantially in different cell lines. This behavior is difficult to predict and must be determined experimentally. These assays were run in Opti-MEM (Figures S10, S11, S13) and repeated with DMEM containing 10% FBS to understand the role of serum in the transfection conditions (Figure 3–6). First, a colorimetric live–dead cell study was performed to assess the cytotoxicity of polyplexes formed from the pMAT-*b*-AEMA and control polymers with pDNA. The 3-(4,5-dimethylthiazol-2-yl)-2,5-diphenyltetrazolium bromide MTT assay is a commonly used viability assay that measures mitochondrial activity.⁴⁰ Cells were exposed to polyplexes in DMEM containing 10% FBS for 4 h then incubated for 48 h prior to running an MTT toxicity assay. Survival of each sample was normalized to a negative control of cells that were exposed to neither pDNA nor polymer (Figure 3).

With HepG2 cells, most samples did not differ in value from the negative control of naïve cells. Only the pAEMA and pMAT-*b*-AEMA-3 polyplexes formulated at an N/P = 7 showed cell survival rates of less than 100%. In the U87 cell line, jetPEI as well as pMAT-*b*-AEMA-3 polyplexes formulated at N/Ps of 14 and 21 showed some toxicity. The pMAT-*b*-AEMA-2 and -3 cell survival values decreased as N/P increased, which matched trends found in previous work with glycopolymer polyplexes. However, none of the pMAT-*b*-AEMA-2 formulations were found to cause a significant decrease in cell survival when compared to naïve

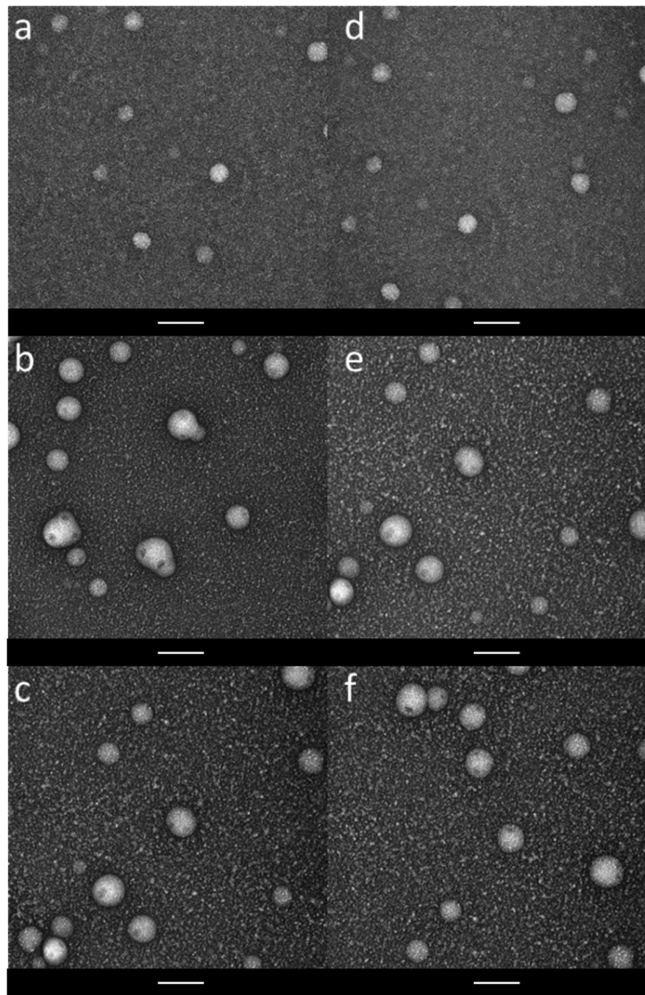


Figure 2. TEM images of polyplexes formulated with (a, d) pMAT-*b*-AEMA-1, (b, e) -2, and (c, f) -3, respectively, at N/P = 10 following negative staining with uranyl acetate (a–c) before lyophilization (d–f) after a single round of lyophilization and reconstitution to original concentration in water. All scale bars are 100 nm.

cells grown without polyplexes present via the Student's *t* test ($p < 0.05$).^{31,41,42} On average, polyplexes formulated with jetPEI at N/P = 5 were between 3 and 48% more toxic to the U87 cells than other polymers tested at higher N/P ratios but were not toxic to HepG2 cells. In both cell lines, the pMAT-*b*-AEMA with shorter AEMA block lengths had equal or higher levels of cell survivability than any of the controls, which also reflects previous work showing the biocompatibility of trehalose polymers.^{31,32,43}

To quantify the amount of plasmid cargo taken up by cells, we fluorescently labeled pDNA with cyanine 5 (Cy 5) prior to transfection. Polyplexes were formulated and exposed to the cells as previously described for the MTT assay. After transfection, cells were washed, collected, and centrifuged to concentrate the cells in solution and analyzed via flow cytometry. After the first run, 2.5 μ L of propidium iodide (PI) was added to the remaining samples in each tube and left to sit for 30 min at room temperature prior to reanalysis. Cells positive for PI were assumed to be dead or dying and were removed from gating. Data were plotted as a percentage of live cells positive for Cy5 (Figure 4).

For the cellular internalization results, all samples were statistically compared to the negative control cells exposed to noncomplexed pDNA. In the HepG2 cells, all but one polyplex formulation had higher Cy5 percentages than DNA alone,

with pAEMA having the highest uptake, followed by pMAT-*b*-AEMA-2, PEG-*b*-AEMA, and jetPEI. pMAT-*b*-AEMA-2 at all three N/P ratios tested had the highest level of polyplex uptake when compared to the other trehalose block-*co*-polycation formulations (and were statistically superior to the positive control jetPEI in HepG2 cells), which correlates with the high gene expression seen in Figure 6 (vide infra). pMAT-*b*-AEMA-1 polyplexes in both cell lines have lower uptake compared with either pMAT-*b*-AEMA-2 or -3 with some formulations barely exceeding background levels.

In the U87 cell line, pMAT-*b*-AEMA-2 polyplexes again had higher cell uptake compared to all other trehalose-containing polymer formulations except for pMAT-*b*-AEMA-3 at N/P = 7. The N/P = 14 and 21 formulations of pMAT-*b*-AEMA-2 and N/P = 7 formulation of pMAT-*b*-AEMA-3 were found to be statistically similar to the positive control jetPEI. While none of the pMAT-*b*-AEMA-2 formulations nor any of the positive controls differed statistically from each other when compared to the cells-only control, an interesting trend appeared in the other samples: both the shortest and longest MAT polymers showed decreased uptake values with an increase in N/P ratio with U87 cells. This trend suggests that more positive charge promotes uptake to a point, then begins to limit uptake. While it was expected that pAEMA polyplexes would have very high uptake due to its high amount of positive charge, it was also predicted to be the most toxic. Surprisingly, we did not observe any effects of cell death with pAEMA polyplexes (at N/P = 7) and thus, this did not impact uptake values. Also, it should be noted that both pMAT-*b*-AEMA-2 and -3 polyplex formulations at N/P = 7 had cell uptake comparable to that of PEG-*b*-AEMA.^{23,44}

Efficiencies of polyplex transfection and uptake of the plasmid cargo were assessed by measuring expression of a luciferase reporter gene. Polyplexes were formed and incubated with cells for 4 h in DMEM containing 10% FBS, followed by an additional incubation period of 48 h to allow for protein expression. Cells were washed, lysed, and the lysate analyzed for luminescence intensity after treatment with luciferin. In Figure 5, luminescence was plotted as relative light units (RLUs) per protein (mg) in each sample to normalize for the number of cells in each well, thus negating differences in expression due to cell death. In both cell lines, jetPEI polyplexes yielded the highest levels of luciferase expression and were statistically higher than the other formulations. Therefore, as shown in Figure 5, we chose to statistically compare the pMAT-*b*-AEMA polyplex formulations to the protein expression yielded by the pAEMA-homopolymer control. In previous work, we have found that polyplexes formed with glucose-containing pMAG-*b*-AEMA exhibited higher transfection efficiency with a shorter length of AEMA when made with siRNA and a longer AEMA block when formulated with plasmid DNA (pDNA).²³ Polyplexes formulated with trehalose-block copolyacids, pMAT-*b*-AEMA, and siRNA also displayed better transfection with a shorter AEMA block than with longer blocks.²⁴ Among the trehalose polyplex formulations studied herein from N/P = 7 to N/P = 21, luciferase expression increased 8 fold in HepG2 cells and 13-fold in U87 cells for pMAT-*b*-AEMA-1 and decreased with N/P with pMAT-*b*-AEMA-3. For pMAT-*b*-AEMA-2 polyplexes, luciferase expression was statistically equivalent from N/P = 7–21 to expression values from pAEMA polyplexes in HepG2 cells. Similarly, gene expression with pMAT-*b*-AEMA-2 polyplexes were also statistically equivalent to that yielded by pAEMA with U87 cells at N/P = 7; however, a decrease in expression was noted with increasing pMAT-*b*-AEMA-2 N/P ratio with this cell type.

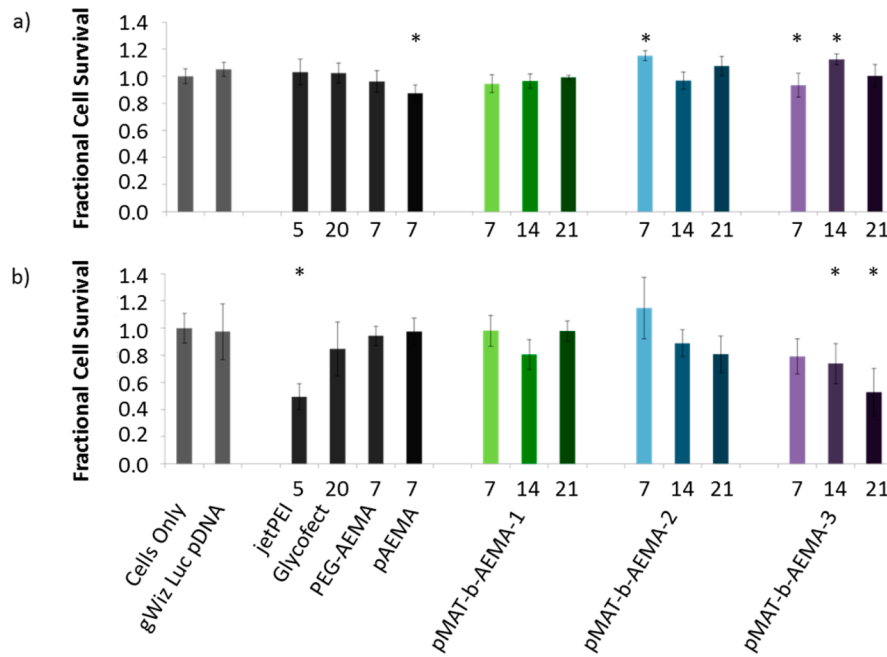


Figure 3. Cell survival MTT Assay following incubation of cells with pMAT-*b*-AEMA (-1, -2, and -3) polyplexes for 48 h in DMEM containing 10% FBS with (a) HepG2 cells and (b) U87 cells. The numbers on the *x*-axis represent the N/P ratio of polyplex formulation for each respective polymer. All results are normalized to a sample containing cells that underwent no treatment and were allowed to proliferate normally for 48 h in DMEM containing 10% FBS. All experiments were performed in triplicate with error bars marking the standard deviation. Samples that were found to be statistically different from cells only survival were marked with an * (according to Student's *t* test with $p < 0.05$).

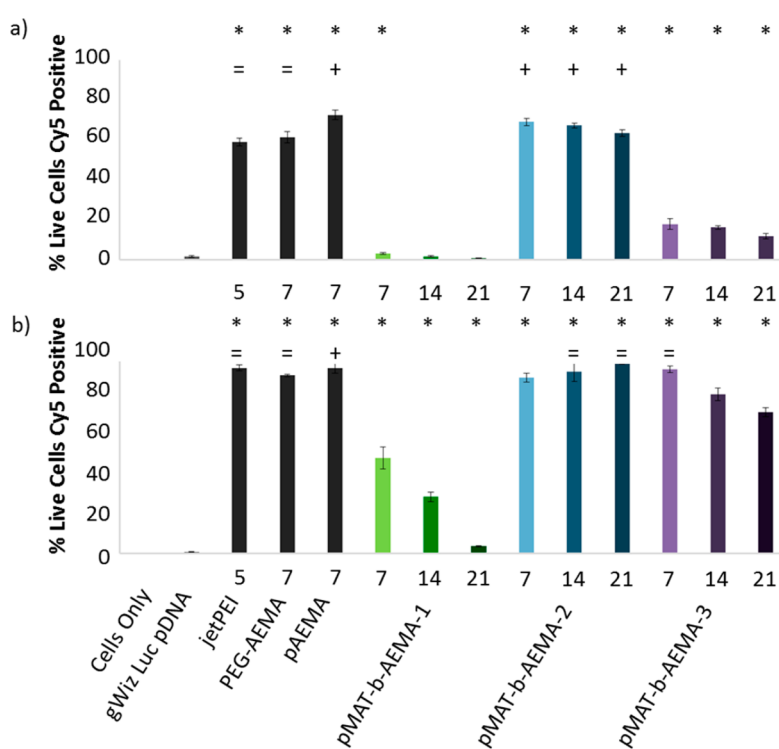


Figure 4. Cellular internalization of pMAT-*b*-AEMA polyplexes formed with Cy5-labeled pDNA and incubated with cells for 4 h in DMEM containing 10% FBS in (a) HepG2 cells and (b) U87 cells. The numbers on the *x*-axis represent the N/P ratio of polyplex formulation for each respective polymer. All experiments were performed in triplicate, where the error bars indicate standard deviation. All samples that were found to be statistically different from DNA only uptake were marked with *. Samples that were found to be significantly higher than the positive control jetPEI are marked with +, and samples found to be statistically equivalent to jetPEI are marked with = (according to Student's *t* test with $p < 0.05$).

The pMAT-*b*-AEMA-2 formulations were the only pMAT-*b*-AEMA-based polyplexes to exhibit luciferase expression at the same level as any of the control polymers. This trend was similar

to the cellular uptake data, again supporting the hypothesis that AEMA (and therefore positive charge) aids cellular internalization and expression to a point. However, with a further increase

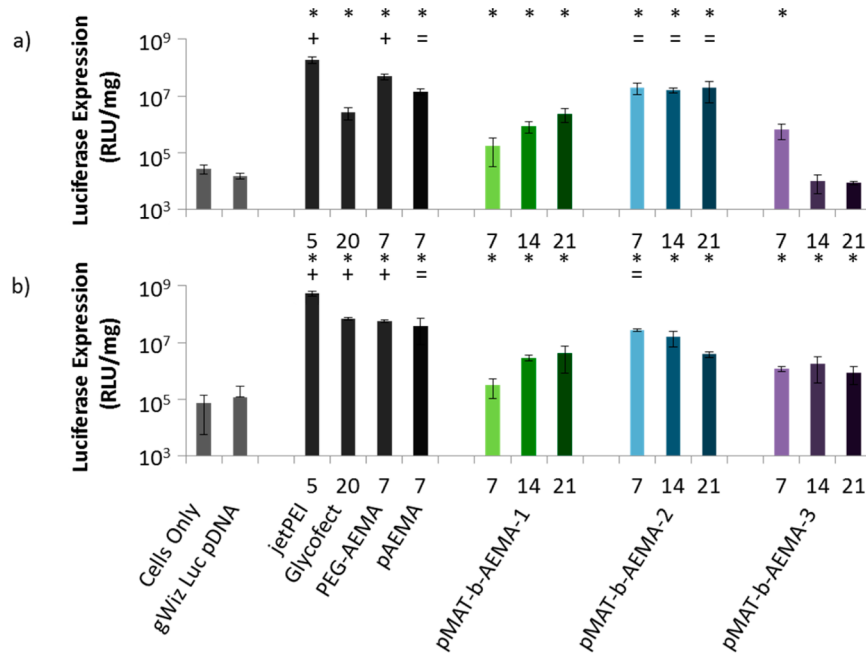


Figure 5. Luminescence of cell lysate following addition of luciferin in (a) HepG2 cells and (b) U87 cells. Cells were incubated with the polyplex formulations for 4 h in DMEM containing 10% FBS followed by an additional 48 h to allow for protein expression. The numbers on the x-axis represent the N/P ratio of polyplex formulation for each respective polymer. All experiments were performed in triplicate with error bars showing standard deviation. All samples that were found to be statistically different from cells only luciferase expression were marked with an *. Samples that were found to be significantly higher than the positive control pAEMA are marked with a +, and samples found to be statistically equivalent to pAEMA are marked with = (according to Student's *t* test with $p < 0.05$).

in the N/P ratio, expression values start to decrease. The decrease could be due to two factors: (i) prevention of the release and transcription of DNA cargo²³ or (ii) by increasing cell membrane permeability to the point of toxicity.^{40,45} Because luminescence RLU are normalized to the amount of cell protein in each sample, cytotoxicity is not enough to account for low expression in either cell line. It is more likely that polyplexes with large AEMA blocks and high ratios of polymer-to-plasmid have higher charge densities that prevent cargo release and transcription,^{23,46} whereas complexes with too little AEMA or too small an N/P ratio could prematurely release DNA prior to nuclear entry.⁴⁷ We were not as concerned with this latter issue because of the stability of the polyplexes that was observed in the DLS data. It should be noted that differences between some samples are not statistically significant, but the general trend that appears in the uptake assays as well as gene expression studies for both cell lines correlates with previous work in the field.^{23,41,44,46}

The pMAT-*b*-AEMA polymers were next tested for their ability to act as a lyoprotectant when complexed with pDNA. pMAT-*b*-AEMA-2, jetPEI, Glycofect, and PEG-*b*-AEMA were used to formulate polyplexes in H₂O and allowed to incubate for 1 h at room temperature. They were immediately frozen in liquid nitrogen and lyophilized to dryness. The resulting powder was then reconstituted with water, allowed to incubate for another hour, and either administered to cells in DMEM + 10% FBS or resubjected to the same lyophilization procedure. Luciferase expression assays were completed as previously described. The expression for each lyophilized polyplex sample was normalized to samples made with the same polymer that had not been lyophilized. Figure 6 shows these data as a percentage of gene expression retained for each round of lyophilization.

Following a single round of lyophilization and reconstitution, only the two polymers containing a sugar moiety, pMAT-*b*-AEMA-2 and Glycofect, retained any ability to transfect U87 cells. pMAT-*b*-AEMA-2 exhibited expression equal to 69% of its initial level while Glycofect was reduced to 4%. It is hypothesized that the pMAT-*b*-AEMA polyplexes form a core–shell structure with the trehalose-containing block coating the external surface of the polyplex, aiding polyplex stability during the lyophilization process. Neither Glycofect nor jetPEI polyplexes contain stabilization layers, leaving these formulations susceptible to aggregation via the lyophilization procedure. Interestingly, the PEG-*b*-AEMA was expected to have a similar polyplex structure (containing a hydrophilic PEG shell coating) to the pMAT-*b*-AEMA-2; however, it did not retain transfection capability

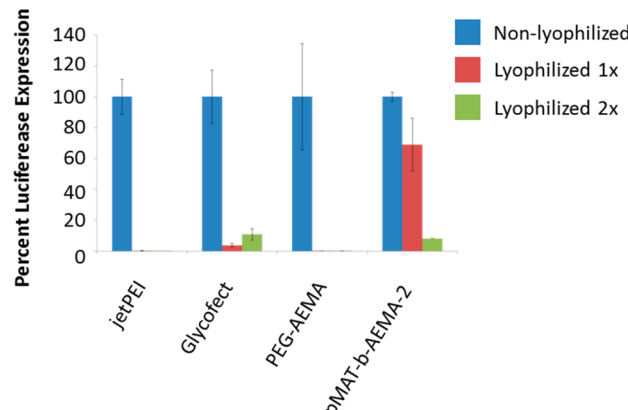


Figure 6. Luciferase expression in U87 cells following transfection with lyophilized polyplexes. JetPEI polyplexes were formulated at N/P = 5, Glycofect polyplexes were formulated at N/P = 20, and PEG-*b*-AEMA and pMAT-*b*-AEMA-2 polyplexes were formulated at N/P = 7. All experiments were performed in triplicate with error bars showing standard deviation.

and Glycofect, retained any ability to transfect U87 cells. pMAT-*b*-AEMA-2 exhibited expression equal to 69% of its initial level while Glycofect was reduced to 4%. It is hypothesized that the pMAT-*b*-AEMA polyplexes form a core–shell structure with the trehalose-containing block coating the external surface of the polyplex, aiding polyplex stability during the lyophilization process. Neither Glycofect nor jetPEI polyplexes contain stabilization layers, leaving these formulations susceptible to aggregation via the lyophilization procedure. Interestingly, the PEG-*b*-AEMA was expected to have a similar polyplex structure (containing a hydrophilic PEG shell coating) to the pMAT-*b*-AEMA-2; however, it did not retain transfection capability

following lyophilization. The trehalose blocks appear to impart a unique protective property to polyplexes for potential lyophilization and storage.

Mouse Studies. Polyplexes formed from pMAT-*b*-AEMA-2 and pDNA had the highest level of gene expression in cultured cells *in vitro* and low toxicity at the three tested N/P ratios; these promising properties led to the selection and examination of this formulation *in vivo*. Murine studies with pMAT-*b*-AEMA-2 were explored for delivering luciferase-encoding pDNA with C57 black 6 (C57BL/6) mice. Tail vein injection was used to probe for biodistribution, toxicity, and transfection of the polyplexes in a living organism.

Mice treated via standard tail vein injections were administered with one of four polyplex formulations in 5% dextrose (D₅W, Table S1) and a fifth control sample of D₅W only. Importantly, with all formulations, all mice survived to the 48 h end point of the study with no noticeable health deterioration. All mice were active and showed no signs of lethargy nor ill health effects after being dosed with up to 490 µg of polymer per mouse (the equivalent of 19.6 mg/kg of polymer/mouse). Following tail vein injection, the mice were then injected peritoneally with luciferin at 24 and 48 h after polyplex injection and imaged using a bioluminescence Xenogen Spectrum CCD camera system. Luciferase gene expression could not be detected either 24 or 48 h after the infusion of polymers. Following the 48 h imaging, all mice were euthanized and the heart, liver, lung, spleen, kidneys, and brain were harvested for analysis by qPCR to determine biodistribution of the pDNA cargo (Table S1).⁴⁸ QPCR analysis revealed a nearly uniform distribution of genetic material throughout the tissues. On a per-cell basis, pDNA was found at a range of 1.1–10 plasmid copies per cell in each organ (values less than or equal to 1.0 copies/cell cannot be resolved from the background). Hydrodynamic injection of 25 µg of pDNA, discussed in further detail below, typically achieves delivery of ~100 plasmids per cell in the liver, leading to significant gene expression.^{36,49} The lower level of genetic material delivered to each of these organs following tail vein injection was insufficient to achieve observable gene expression.

Multiple cyanine fluorophores, including Cy7, have been used successfully to tag DNA cargos for *in vivo* imaging.^{50–52}

Using cyanine-3 labeled siRNA, Davis and co-workers have shown that tail vein-injected polyplexes begin urinary clearance within 6 min.⁵² Here, to determine if the polymer and pDNA reached the tissues with similar distributions (indicative of intact polyplexes), we fluorescently labeled pMAT-*b*-AEMA-2 with Cy7 via amine-NHS coupling chemistry. Polyplexes were then formulated with Cy7-pMAT-*b*-AEMA-2 polymer and 25 µg of pDNA at an N/P = 7 and administered to mice via tail vein injections. Animals were imaged 15 min postinjection, euthanized, and the organs were harvested and imaged (Figure 7).

Fluorescence was observed in the liver, spleen, kidneys, and lungs of the mice injected with the Cy7-labeled pMAT-*b*-AEMA-2 (Figure 7). Fluorescence was not observed in the blood, indicating that the polymers/polyplexes had fully cleared the bloodstream (at the detectable level). As expected, the organs from the naïve mouse also did not show fluorescence, indicating that the fluorescence visualized in the experimental mice arose from the Cy7-labeled polymer and not from background fluorescence from the tissues.

Collectively, these data show that the concentration of plasmid delivered to each organ was insufficient to observe significant gene expression in the mice when delivered through a standard tail vein injection. Thus, a hydrodynamic injection technique was then examined to promote plasmid delivery specifically to the liver, wherein a large volume of DNA solution, typically 2 mL in a 20 g mouse, is infused in 4–8 s.³⁶ More than 99% of the gene can be localized to the liver⁵³ as the high pressure appears to expand the liver endothelium promoting liver cell internalization and gene expression.^{53–55} Typically, naked plasmid DNA is used with this injection technique and results in high signals of gene expression, ~1 × 10¹⁰ to 1 × 10¹¹ RLUs, in the liver when the firefly luciferase gene is placed behind a strong promoter such as the hybrid b-actin/cytomegalovirus (CAGGS) synthetic promoter (Scheme 1). The large volume injected, combined with the high pressure, has been found to strain the mouse, especially the cardiac system^{56,57} and the liver; it takes 24 to 48 h for the liver to recover from the injection.^{1,4,5} However, while direct scale up of systemic hydrodynamic injection to larger mammals resulting in sustained transgene expression has yet to be achieved,⁵⁸

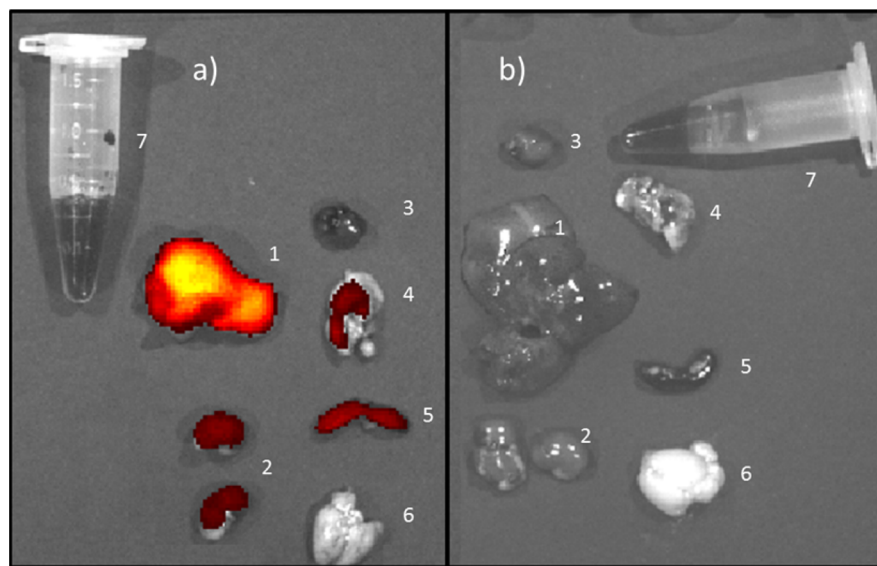


Figure 7. Fluorescence image of organs harvested from (a) a mouse injected with a Cy-7 pMAT-*b*-AEMA-2 polyplex and (b) a naïve mouse measured with a Xenogen Spectrum CCD camera system. Excised tissues: 1, liver; 2, kidney; 3, heart; 4, lung; 5, spleen; 6, brain; 7, blood.

it may be potentially translatable if the high pressure injection is isolated only to the organ of interest and formulation of DNA into polyplexes could improve delivery and gene expression. For example, Itaka and co-workers were able to perform a hydrodynamic injection directed to skeletal muscle by injecting into a limb isolated with a tourniquet.⁵⁹ DNA delivered as a polyplex formulated from a PEG-poly-L-lysine cationic block copolymer showed increased expression and DNA lifetime in the tissue when compared to similar injections performed with naked pDNA.⁵⁹ Nakamura and co-workers performed hydrodynamic injection followed by a luciferase assay on excised liver tissue and found that polyplexes formed with jetPEI yielded higher luminescence than naked pDNA.⁶⁰

Herein, Glycofect, jetPEI, and pMAT-*b*-AEMA-2 were used to deliver 10 µg of pDNA via hydrodynamic injection and compared to naked pDNA as a control (Table 2). All mice

Table 2. Formulations and Luciferase Expression of Mice Treated with Polyplexes via Hydrodynamic Injections^a

sample	formulation	dose pDNA (µg)	luminescence 24 h (photons/s)	luminescence 48 h (photons/s)
Glycofect	N/P: 3	10	2.50×10^9 *	1.39×10^9 *
jetPEI	N/P: 7	10	3.70×10^7 *	8.52×10^7 *
jetPEI	N/P: 3	25	4.53×10^8 *	1.64×10^8 *
pMAT- <i>b</i> -AEMA-2	N/P: 3	10	4.39×10^{10}	2.29×10^{10}
pDNA	N/A	10	3.95×10^{10}	8.93×10^9

^aLuminescence levels were averaged from the values obtained from 3 mice in each data set and are reported in photons/s. The logarithm of each measurement was calculated and samples that were found to be statistically different from pMAT-*b*-AEMA-2 were marked with an * (according to Student's t-test with $p < 0.05$).

survived the high-pressure injections. To analyze gene expression, the mice were injected peritoneally with luciferin at 24 and 48 h and imaged with a Xenogen system (Figure 8). Interestingly, jetPEI, despite being the most effective delivery vehicle in tissue culture, showed the lowest level of luciferase expression in the liver of all tested formulations via live-animal imaging. The luminescence level was found to be 2–3 orders of magnitude below that of the naked pDNA. Even when the amount of DNA was more than doubled to 25 µg, the luminescence level was still 1 to 2 orders of magnitude below that of the control. Glycofect was the more effective of the commercially available transfection agents but still performed an order of magnitude below the control. Polyplexes formed with pMAT-*b*-AEMA-2 transfected at a higher level than either of the commercially available polymers and maintained the same level of gene expression as the naked pDNA control. Taken together, these results show that pMAT-*b*-AEMA-2 polyplexes are capable of delivering DNA that can subsequently be expressed *in vivo* with minor toxicity.

It appears that the majority of the pDNA was delivered to the liver because of the high levels of gene expression observed. Polyplexes were again formed using the Cy7-labeled pMAT-*b*-AEMA-2 and injected hydrodynamically to verify delivery of intact polyplexes to the liver and understand polymer distribution with this high pressure delivery technique. Animals were injected, imaged 15 min post-injection, euthanized, and the organs were harvested and imaged (Figure 9). The liver was the only organ to show significant fluorescence, indicating that the polyplexes stay intact during the hydrodynamic experiment as polymer and pDNA are localized to the liver and are responsible for yielding high levels of gene expression.

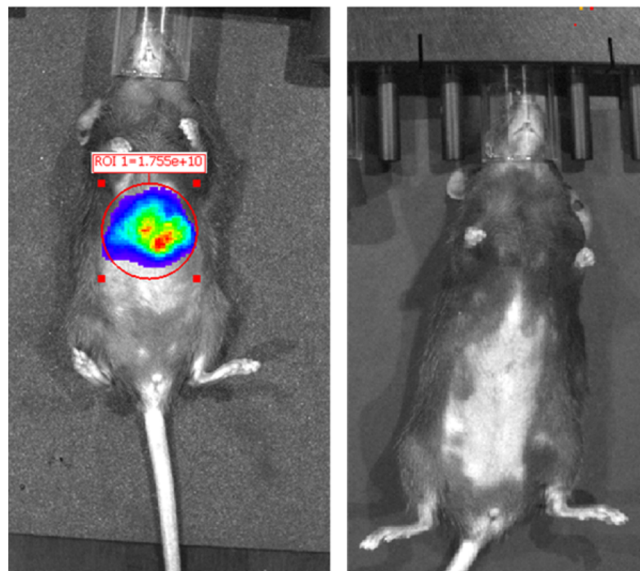


Figure 8. Luminescence images of a hydrodynamically injected mouse with pMAT-*b*-AEMA-2 and pDNA encoding for luciferase polyplexes following treatment with luciferin (left) and control mouse hydrodynamically injected with D₅W solution only (right) measured with a Xenogen Spectrum CCD camera system. The images shown are representative to that observed for $N = 3$ replicates.

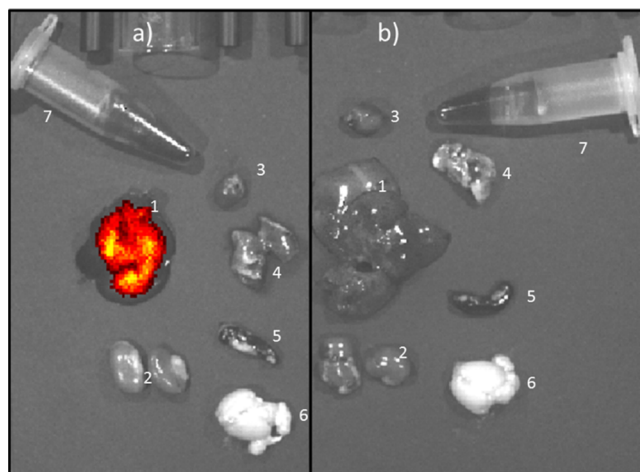


Figure 9. Fluorescence image of organs harvested from (a) a mouse hydrodynamically injected with a Cy-7 pMAT-*b*-AEMA-2 polyplex and (b) a naïve mouse measured with a Xenogen Spectrum CCD camera system. Tissues: 1, liver; 2, kidney; 3, heart; 4, lung; 5, spleen; 6, brain; 7, blood. The images shown are representative to that observed for $N = 3$ replicates.

CONCLUSION

Trehalose-containing cationic block copolymers were synthesized and their colloidal stabilization and gene delivery properties were examined in detail in vitro and in vivo. The pMAT-*b*-AEMA polymers bound pDNA and remained stable over time even in the presence of serum. Studies in tissue-cultured cells, however, indicated that both the pAEMA block length and polymer–pDNA ratio are important factors in determining toxicity, cellular uptake, and gene expression.

Overall, the pMAT-*b*-AEMA polymers demonstrated low toxicity, high levels of luciferase expression, and were also able to harness the unique property of trehalose as a lyoprotectant upon freeze-drying and resuspension, prompting *in vivo* studies of

these formulations.²⁴ To test the biodistribution and toxicity of these trehalose-stabilized polyplexes *in vivo*, we selected pMAT-*b*-AEMA-2 for murine studies.

The mice appeared to suffer no ill health effects after being dosed with up to 490 µg of polymer per mouse (the equivalent of 19.6 mg/kg of polymer/mouse). Quantitative PCR studies were conducted to measure the plasmid amount in six major organs. The amount of plasmid present was very low, especially when compared to plasmid levels in the liver following hydrodynamic infusion.^{36,49} The low level of polyplex uptake by all tissues was insufficient to achieve detectable levels of luciferase gene expression. The widespread and roughly equal distribution of the polyplexed plasmid suggested that the trehalose polyplexes were colloidally stable during circulation and offer an excellent design motif for further *in vivo* delivery experiments. To determine the *in vivo* stability of the polyplexes (whether the polymer retained its cargo upon delivery), we fluorescently tagged the polymer and imaged the mice and their organs. After 15 min of polyplex circulation, we detected fluorescence in the organs where pDNA was found but not in the blood, which was consistent with results that injected polyplexes are cleared into the urine within 6 min.⁵²

A second injection method was then used to bypass extended circulation in the blood as a physical means to target polyplex delivery to a specific tissue. Accordingly, we performed a hydrodynamic infusion to force the majority of polyplexes to the liver,^{53–55} which resulted in significant luciferase expression. Indeed, gene expression was comparable to that seen in previous work with diseased mouse models,⁵⁴ suggesting that genes coding for therapeutic proteins would also be expressed at high levels when complexed with pMAT-*b*-AEMA-2. Because of the large volumes required to perform hydrodynamic injection, it is difficult to expand the use of this delivery technique into higher mammal models.^{58–60} Catheters are being explored to localize the high pressure to targeted tissues of interest, yet it is still difficult to achieve sufficient pressure levels needed to promote successful naked plasmid delivery and gene expression *in vivo*. Polyplexing plasmids could offer a method to reduce the injection volume and pressure needed to maintain significant gene expression. To this end, we show that polyplexing pDNA does not appear to prohibit its delivery/expression through *in vivo* hydrodynamic delivery methods (in fact, higher gene expression was observed) and shows promise to offer a way to formulate plasmids for direct catheter-based tissue administration. Overall, this work demonstrates the unique properties of trehalose for stabilizing polyplex formulations for lyophilization and delivery *in vivo*, important metrics for advancing new vehicles for clinical gene therapy applications. Future work is aimed at introducing these polyplex formulations with therapeutic genes by isolating hydrodynamic infusions to the liver of animal models.

ASSOCIATED CONTENT

Supporting Information

The Supporting Information is available free of charge on the ACS Publications website at DOI: [10.1021/acsbiomaterials.5b00312](https://doi.org/10.1021/acsbiomaterials.5b00312).

Detailed experimental procedures, chemical characterization, additional *in vitro* characterization, and PCR analysis of plasmid delivery to major organs ([PDF](#))

AUTHOR INFORMATION

Corresponding Author

*E-mail: treineke@umn.edu.

Present Addresses

[‡]M.C. is currently Department of Physical Sciences, Nicholls State University, Thibodaux, LA, 70310.

[§]Y.W. is currently at University of Chicago, Department of Surgery, 5812 S. Ellis Ave., Chicago, IL, 60637.

Notes

The authors declare no competing financial interest.

ACKNOWLEDGMENTS

We acknowledge funding of this project by the NIH Director's New Innovator Program (DP2OD006669) and the Camille and Henry Dreyfus Foundation to TMR. We acknowledge the use of UMN Bruker NMR spectrometers through the following statement: Research reported in this publication was supported by the Office of the Director, National Institutes of Health of the National Institutes of Health under Award S10OD011952. We acknowledge the financial support of NIH grants 1R01DK082516 and P01HD32652 to PH. The content is solely the responsibility of the authors and does not necessarily represent the official views of the National Institutes of Health. All animal studies were performed under the IACUC Protocol #1202A09921 (PI: Hackett).

REFERENCES

- (1) Reid, T.; Galanis, E.; Abbruzzese, J.; Sze, D.; Andrews, J.; Romel, L.; Hatfield, M.; Rubin, J.; Kirn, D. Intra-arterial administration of a replication-selective adenovirus (dl1520) in patients with colorectal carcinoma metastatic to the liver: a phase I trial. *Gene Ther.* **2001**, *8*, 1618–1626.
- (2) Roth, J. A.; Cristiano, R. J. Gene therapy for cancer: what have we done and where are we going? *J. Natl. Cancer Inst.* **1997**, *89*, 21–39.
- (3) Zhang, Y.; Zheng, M.; Kissel, T.; Agarwal, S. Design and biophysical characterization of bioreponsive degradable poly(dimethylaminoethyl methacrylate) based polymers for *in vitro* DNA transfection. *Biomacromolecules* **2012**, *13*, 313–322.
- (4) Liu, F.; Huang, L. Development of non-viral vectors for systemic gene delivery. *J. Controlled Release* **2002**, *78*, 259–266.
- (5) Ginn, S. L.; Alexander, I. E.; Edelstein, M. L.; Abedi, M. R.; Wixon, J. Gene therapy clinical trials worldwide to 2012 - an update. *J. Gene Med.* **2013**, *15*, 65–77.
- (6) Kay, M. A. State-of-the-art gene-based therapies: the road ahead. *Nat. Rev. Genet.* **2011**, *12*, 316–328.
- (7) Verma, I. M. Gene therapy that works. *Science* **2013**, *341*, 853–855.
- (8) Wilson, J. M. Genetic diseases, immunology, viruses, and gene therapy. *Hum. Gene Ther.* **2014**, *25*, 257–261.
- (9) Vorburger, S. A.; Hunt, K. K. Adenoviral gene therapy. *Oncologist* **2002**, *7*, 46–59.
- (10) Yin, H.; Kanasty, R. L.; Eltoukhy, A. A.; Vegas, A. J.; Dorkin, J. R.; Anderson, D. G. Non-viral vectors for gene-based therapy. *Nat. Rev. Genet.* **2014**, *15*, 541–555.
- (11) Zhang, Y.; Satterlee, A.; Huang, L. *In vivo* gene delivery by nonviral vectors: overcoming hurdles? *Mol. Ther.* **2012**, *20*, 1298–1304.
- (12) Hackett, P. B.; Largaespada, D. A.; Cooper, L. J. N. A transposon and transposase system for human application. *Mol. Ther.* **2010**, *18*, 674–683.
- (13) Gary, D. J.; Lee, H.; Sharma, R.; Lee, J.-S.; Kim, Y.; Cui, Z. Y.; Jia, D.; Bowman, V. D.; Chipman, P. R.; Wan, L.; Zou, Y.; Mao, G.; Park, K.; Herbert, B.-S.; Konieczny, S. F.; Won, Y.-Y. Influence of nano-carrier architecture on *in vitro* siRNA delivery performance and *in vivo* biodistribution: polyplexes vs micelleplexes. *ACS Nano* **2011**, *5*, 3493–3505.
- (14) Karmali, P. P.; Simberg, D. Interactions of nanoparticles with plasma proteins: implication on clearance and toxicity of drug delivery systems. *Expert Opin. Drug Delivery* **2011**, *8*, 343–357.
- (15) Knop, K.; Hoogenboom, R.; Fischer, D.; Schubert, U. S. Poly(ethylene glycol) in drug delivery: pros and cons as well as potential alternatives. *Angew. Chem., Int. Ed.* **2010**, *49*, 6288–6308.

- (16) Caliceti, P.; Veronese, F. M. Pharmacokinetic and biodistribution properties of poly(ethylene glycol)-protein conjugates. *Adv. Drug Delivery Rev.* **2003**, *55*, 1261–1277.
- (17) Dewachter, P.; Mouton-Faivre, C. Anaphylaxis to macrogol 4000 after a parenteral corticoid injection. *Allergy* **2005**, *60*, 705–706.
- (18) Chanan-Khan, A.; Szebeni, J.; Savay, S.; Liebes, L.; Rafique, N. M.; Alving, C. R.; Muggia, F. M. Complement activation following first exposure to pegylated liposomal doxorubicin (Doxil): possible role in hypersensitivity reactions. *Ann. Oncol.* **2003**, *14*, 1430–1437.
- (19) Szebeni, J. Complement activation-related pseudoallergy: a new class of drug-induced acute immune toxicity. *Toxicology* **2005**, *216*, 106–121.
- (20) Ishida, T.; Harada, M.; Wang, X. Y.; Ichihara, M.; Irimura, K.; Kiwada, H. Accelerated blood clearance of PEGylated liposomes following preceding liposome injection: Effects of lipid dose and PEG surface-density and chain length of the first-dose liposomes. *J. Controlled Release* **2005**, *105*, 305–317.
- (21) Ishida, T.; Kashima, S.; Kiwada, H. The contribution of phagocytic activity of liver macrophages to the accelerated blood clearance (ABC) phenomenon of PEGylated liposomes in rats. *J. Controlled Release* **2008**, *126*, 162–165.
- (22) Ishida, T.; Kiwada, H. Accelerated blood clearance (ABC) phenomenon upon repeated injection of PEGylated liposomes. *Int. J. Pharm.* **2008**, *354*, 56–62.
- (23) Smith, A. E.; Sizovs, A.; Grandinetti, G.; Xue, L.; Reineke, T. M. Diblock glycopolymers promote colloidal stability of polyplexes and effective pDNA and siRNA delivery under physiological salt and serum conditions. *Biomacromolecules* **2011**, *12*, 3015–3022.
- (24) Sizovs, A.; Xue, L.; Tolstyka, Z. P.; Ingle, N. P.; Wu, Y. Y.; Cortez, M.; Reineke, T. M. Poly(trehalose): sugar-coated nanocomplexes promote stabilization and effective polyplex-mediated siRNA delivery. *J. Am. Chem. Soc.* **2013**, *135*, 15417–15424.
- (25) Streeter, J. G. Accumulation of alpha,alpha-trehalose by Rhizobium bacteria and bacteroids. *J. Bacteriol.* **1985**, *164*, 78–84.
- (26) Teramoto, N.; Sachinvala, N. D.; Shibata, M. Trehalose and trehalose-based polymers for environmentally benign, biocompatible and bioactive materials. *Molecules* **2008**, *13*, 1773–1816.
- (27) Ramløv, H.; Westh, P. Survival of the cryptobiotic eutardigrade *Adorybiotus coronifer* during cooling to -196°C : effect of cooling rate, trehalose level, and short-term acclimation. *Cryobiology* **1992**, *29*, 125–130.
- (28) Somme, L. Anhydrobiosis and cold tolerance in tardigrades. *Eur. J. Entomol.* **1996**, *93*, 349–357.
- (29) Ohtake, S.; Wang, Y. J. Trehalose: current use and future applications. *J. Pharm. Sci.* **2011**, *100*, 2020–2053.
- (30) Anderson, K.; Sizovs, A.; Cortez, M.; Waldron, C.; Haddleton, D. M.; Reineke, T. M. Effects of trehalose polycation end-group functionalization on plasmid DNA uptake and transfection. *Biomacromolecules* **2012**, *13*, 2229–2239.
- (31) Srinivasachari, S.; Liu, Y.; Prevete, L. E.; Reineke, T. M. Effects of trehalose click polymer length on pDNA complex stability and delivery efficacy. *Biomaterials* **2007**, *28*, 2885–2898.
- (32) Srinivasachari, S.; Liu, Y.; Zhang, G.; Prevete, L.; Reineke, T. M. Trehalose click polymers inhibit nanoparticle aggregation and promote pDNA delivery in serum. *J. Am. Chem. Soc.* **2006**, *128*, 8176–8184.
- (33) Mancini, R. J.; Lee, J.; Maynard, H. D. Trehalose glycopolymers for stabilization of protein conjugates to environmental stressors. *J. Am. Chem. Soc.* **2012**, *134*, 8474–8479.
- (34) Podetz-Pedersen, K. M.; Vezys, V.; Somia, N. V.; Russell, S. J.; McIvor, R. S. Cellular immune response against firefly luciferase after sleeping beauty-mediated gene transfer *in vivo*. *Hum. Gene Ther.* **2014**, *25*, 955–965.
- (35) Belur, L. R.; Podetz-Pedersen, K.; Frandsen, J.; McIvor, R. S. Lung-directed gene therapy in mice using the nonviral Sleeping Beauty transposon system. *Nat. Protoc.* **2007**, *2*, 3146–3152.
- (36) Bell, J. B.; Podetz-Pedersen, K. M.; Aronovich, E. L.; Belur, L. R.; McIvor, R. S.; Hackett, P. B. Preferential delivery of the Sleeping Beauty transposon system to livers of mice by hydrodynamic injection. *Nat. Protoc.* **2007**, *2*, 3153–3165.
- (37) Wright, J. C.; Westh, P.; Ramløv, H. Cryptobiosis in tardigrada. *Biol. Rev.* **1992**, *67*, 1–29.
- (38) Li, X.; Mya, K. Y.; Ni, X.; He, C.; Leong, K. W.; Li, J. Dynamic and static light scattering studies on self-aggregation behavior of biodegradable amphiphilic poly(ethylene oxide)-poly[(R)-3-hydroxybutyrate]-poly(ethylene oxide) triblock copolymers in aqueous solution. *J. Phys. Chem. B* **2006**, *110*, 5920–5926.
- (39) Nielsen, P. E. In *DNA-Protein Interactions: Principles and Protocols*, third ed.; Moss, T., Leblanc, B., Eds.; Humana Press: New York, 2009; p 87.
- (40) Grandinetti, G.; Ingle, N. P.; Reineke, T. M. Interaction of poly(ethylenimine)-DNA polyplexes with mitochondria: implications for a mechanism of cytotoxicity. *Mol. Pharmaceutics* **2011**, *8*, 1709–1719.
- (41) Ahmed, M.; Narain, R. The effect of polymer architecture, composition, and molecular weight on the properties of glycopolymer-based non-viral gene delivery systems. *Biomaterials* **2011**, *32*, 5279–5290.
- (42) Lee, C.-C.; Liu, Y.; Reineke, T. M. A general structure-bioactivity relationship for poly(glycoamidoamines)s: amine density and branching affects cytotoxicity and pDNA delivery efficiency. *Bioconjugate Chem.* **2008**, *19*, 428–440.
- (43) Reineke, T. M.; Davis, M. E. Structural effects of carbohydrate-containing polycations on gene delivery. 1. Carbohydrate size and its distance from charge centers. *Bioconjugate Chem.* **2003**, *14*, 247–254.
- (44) Li, H.; Cortez, M. A.; Phillips, H. R.; Wu, Y.; Reineke, T. M. Poly(2-deoxy-2-methacrylamido glucopyranose)-b-Poly(methacrylate amine)s: optimization of diblock glycopolycations for nucleic acid delivery. *ACS Macro Lett.* **2013**, *2*, 230–235.
- (45) Grandinetti, G.; Smith, A. E.; Reineke, T. M. Membrane and nuclear permeabilization by polymeric pDNA vehicles: efficient method for gene delivery or mechanism of cytotoxicity? *Mol. Pharmaceutics* **2012**, *9*, 523–538.
- (46) Hwang, S. J.; Bellocq, N. C.; Davis, M. E. Effects of structure of beta-cyclodextrin-containing polymers on gene delivery. *Bioconjugate Chem.* **2001**, *12*, 280–290.
- (47) Buckwalter, D. J.; Sizovs, A.; Ingle, N. P.; Reineke, T. M. MAG versus PEG: incorporating a Poly(MAG) layer to promote colloidal stability of nucleic acid/“click cluster” complexes. *ACS Macro Lett.* **2012**, *1*, 609–613.
- (48) VanGuilder, H. D.; Vrana, K. E.; Freeman, W. M. Twenty-five years of quantitative PCR for gene expression analysis. *BioTechniques* **2008**, *44*, 619–626.
- (49) Aronovich, E. L.; Bell, J. B.; Belur, L. R.; Gunther, R.; Koniar, B.; Erickson, D. C. C.; Schachern, P. A.; Matisse, I.; McIvor, R. S.; Whitley, C. B.; Hackett, P. B. Prolonged expression of a lysosomal enzyme in mouse liver after *Sleeping Beauty* transposon-mediated gene delivery: implications for non-viral gene therapy of mucopolysaccharidoses. *J. Gene Med.* **2007**, *9*, 403–415.
- (50) Cieslewicz, M.; Tang, J.; Yu, J. L.; Cao, H.; Zavaljevski, M.; Motoyama, K.; Lieber, A.; Raines, E. W.; Pun, S. H. Targeted delivery of proapoptotic peptides to tumor-associated macrophages improves survival. *Proc. Natl. Acad. Sci. U. S. A.* **2013**, *110*, 15919–15924.
- (51) Lin, X.; Zhu, H.; Luo, Z.; Hong, Y.; Zhang, H.; Liu, X.; Ding, H.; Tian, H.; Yang, Z. Near-infrared fluorescence imaging of non-Hodgkin’s lymphoma CD20 expression using Cy7-conjugated obinutuzumab. *Mol. Imaging Biol.* **2014**, *16*, 877–887.
- (52) Zuckerman, J. E.; Choi, C. H. J.; Han, H.; Davis, M. E. Polycation-siRNA nanoparticles can disassemble at the kidney glomerular basement membrane. *Proc. Natl. Acad. Sci. U. S. A.* **2012**, *109*, 3137–3142.
- (53) Podetz-Pedersen, K. M.; Bell, J. B.; Steele, T. W. J.; Wilber, A.; Shier, W. T.; Belur, L. R.; McIvor, R. S.; Hackett, P. B. Gene expression in lung and liver after intravenous infusion of polyethylenimine complexes of *Sleeping Beauty* transposons. *Hum. Gene Ther.* **2010**, *21*, 210–220.
- (54) Aronovich, E. L.; Bell, J. B.; Khan, S. A.; Belur, L. R.; Gunther, R.; Koniar, B.; Schachern, P. A.; Parker, J. B.; Carlson, C. S.; Whitley, C. B.; McIvor, R. S.; Gupta, P.; Hackett, P. B. Systemic correction of storage

disease in MPS I NOD/SCID mice using the sleeping beauty transposon system. *Mol. Ther.* **2009**, *17*, 1136–1144.

(55) Aronovich, E. L.; McIvor, R. S.; Hackett, P. B. The Sleeping Beauty transposon system: a non-viral vector for gene therapy. *Hum. Mol. Genet.* **2011**, *20*, R14–R20.

(56) Sawyer, G. J.; Dong, X.; Whitehorne, M.; Grehan, A.; Seddon, M.; Shah, A. M.; Zhang, X.; Fabre, J. W. Cardiovascular function following acute volume overload for hydrodynamic gene delivery to the liver. *Gene Ther.* **2007**, *14*, 1208–1217.

(57) Zhang, G.; Gao, X.; Song, Y. K.; Vollmer, R.; Stoltz, D. B.; Gasiorowski, J. Z.; Dean, D. A.; Liu, D. Hydroporation as the mechanism of hydrodynamic delivery. *Gene Ther.* **2004**, *11*, 675–682.

(58) Hackett, P. B.; Aronovich, E. L.; Hunter, D.; Urness, M.; Bell, J. B.; Kass, S. J.; Cooper, L. J. N.; McIvor, S. Efficacy and safety of Sleeping Beauty transposon-mediated gene transfer in preclinical animal studies. *Curr. Gene Ther.* **2011**, *11*, 341–349.

(59) Itaka, K.; Osada, K.; Morii, K.; Kim, P.; Yun, S. H.; Kataoka, K. Polyplex nanomicelle promotes hydrodynamic gene introduction to skeletal muscle. *J. Controlled Release* **2010**, *143*, 112–119.

(60) Nakamura, S.; Maehara, T.; Watanabe, S.; Ishihara, M.; Sato, M. Improvement of hydrodynamics-based gene transfer of nonviral DNA targeted to murine hepatocytes. *BioMed Res. Int.* **2013**, *2013*, 928790.